Photoluminescence dynamics and reduced Auger recombination in Si$_{1-x}$Ge$_x$/Si superlattices under high-density photoexcitation

Takeshi Tayagaki,[1] Susumu Fukatsu,[2] and Yoshihiko Kanemitsu[1,3,*]

[1]*Institute for Chemical Research, Kyoto University, Uji, Kyoto 611-0011, Japan*
[2]*Graduate School of Arts and Sciences, The University of Tokyo, Tokyo 153-8902, Japan*
[3]*Photonics and Electronics Science and Engineering Center, Kyoto University, Kyoto 615-8510, Japan*

Optical gain and stimulated emission processes in Si nanostructures are controlled by the dynamics of high-density carriers. Here, we report photoluminescence (PL) dynamics and multiexciton recombination in Si$_{1-x}$Ge$_x$/Si superlattices (SLs) under high-density excitation. Saturation of the PL intensity and rapid PL decay are observed as the excitation laser intensity is increased. These phenomena occur due to nonradiative Auger recombination of the electron-hole pairs. We find that the Auger process in Si$_{1-x}$Ge$_x$/Si SLs is less pronounced than that in the Si$_{1-x}$Ge$_x$/Si single quantum wells. Our results show that coupled nanostructures have an advantage in efficient light emission and the control of many-body carrier dynamics.

Since the first observation of efficient visible photoluminescence (PL) in porous silicon,[1] there have been numerous reports of attempts to increase light-emission efficiency, optical gain, and stimulated light emission in various types of Si nanostructures.[2–10] Quantum confinement of Si nanostructures increases the radiative recombination rate and hence the PL efficiency, while spatial confinement decreases the nonradiative recombination rate.[4] Recently, spatially and quantum-confined Si/SiO$_2$ quantum well nanostructures have been used to study high-density electron-hole plasmas (EHPs) and droplets.[11–13] The dynamics of high-density carriers in Si-based nanostructures plays an essential role in light emission, optical gain processes, free-carrier absorption, and nonlinear optical responses in Si nanostructures and Si-based lasers.[2,9] The nonradiative Auger recombination of photocarriers controls the PL intensity and the electron-hole density under high-density excitation, in bulk Si crystals and Si-based nanostructures as well as in various kinds of semiconductor nanostructures such as nanocrystals, quantum rods, and carbon nanotubes.[14–16] The Auger recombination process in controlled Si nanostructures is crucial to our understanding of the physics of highly dense carriers in other semiconductor nanostructures as well as in Si-based lasers.

The Si$_{1-x}$Ge$_x$/Si heterostructures and quantum well structures are compatible with standard Si processing technology.[2,17,18] The PL from EHPs in Si$_{1-x}$Ge$_x$/Si quantum wells has been observed under high-density excitation using time-integrated PL measurements.[19] However, the dynamic properties of PL under high-density conditions at low temperatures are not clear yet. The Si$_{1-x}$Ge$_x$/Si heterostructures provide a unique opportunity to investigate high-density electron-hole carriers in controlled spatially confined systems.

In this Rapid Communication, we report PL dynamics in Si$_{1-x}$Ge$_x$/Si superlattices (SLs) and single-quantum wells (SQWs) under high-density photoexcitation at low temperatures. The PL spectra and PL decay measurements indicate that nonradiative Auger recombination dominates the luminescence properties. The dependence of the PL spectra on excitation intensity shows that the Auger recombination rate

is suppressed in Si$_{1-x}$Ge$_x$/Si SLs as compared to that in the Si$_{1-x}$Ge$_x$/Si SQWs.

The samples are 99-period gas source molecular-beam epitaxy (MBE)-grown strained Si$_{1-x}$Ge$_x$/Si type-II SL with x =0.15.[20] The well and barrier widths were L_z=3 nm and L_b=3.6 nm, respectively. The well width, which is smaller than the exciton Bohr radius (approximately 6 nm),[21] determines the PL peak energies. The small barrier width (L_b =3.6 nm) allows the electron-hole pairs in the quantum wells to couple.[22] A Si$_{0.82}$Ge$_{0.18}$/Si SQW with well width L_z=2.7 nm was also used for comparison. The second harmonics of a 150 fs Ti:sapphire laser (3.1 eV) and cw gallium nitride laser (3.0 eV) were used as the excitation light sources. Typical spot sizes of these pulse and cw excitation light sources are 20 and 2 μm, respectively. The time-integrated PL spectra were measured using a liquid nitrogen-cooled InGaAs array detector. The PL lifetime was measured using a gated-photon counting system with a photomultiplier.

Figure 1(a) shows the PL spectra in the Si$_{0.85}$Ge$_{0.15}$/Si SL at different temperatures. Three prominent PL peaks appear, which are assigned to the transverse-optical (TO) and
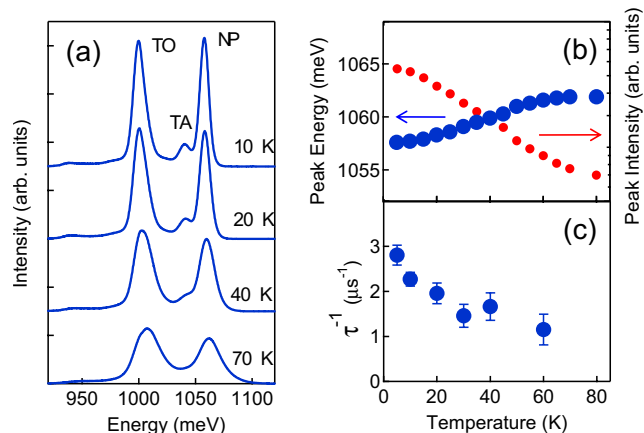

FIG. 1. (Color online) (a) PL spectra under cw excitation measured at 10, 20, 40, and 70 K. Temperature dependence of the (b) peak energies, peak intensities, and (c) PL decay rate of the NP line.
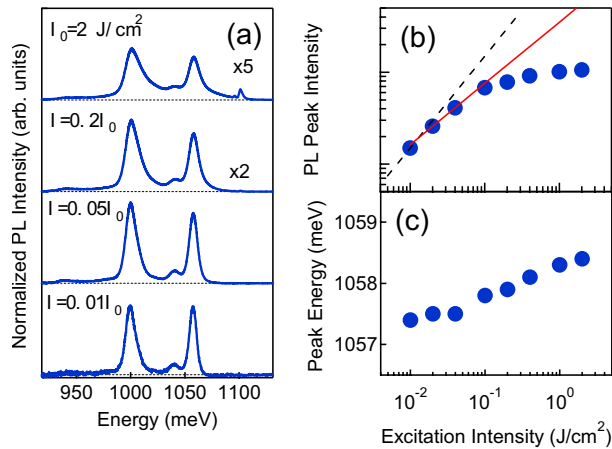
FIG. 2. (Color online) (a) Time-integrated PL spectra under different excitation intensities. (b) The PL peak intensity at 1057 meV and (c) peak energy as a function of the excitation intensity. The broken line shows the linear power dependence. The solid line shows the power dependence of the PL intensity in the case of radiative bimolecular recombination as controlled by nonradiative Auger recombination ($I_{PL} \propto I_{exc}^{2/3}$).

transverse-acoustic (TA) phonon-assisted transitions and the no-phonon-assisted (NP) transition.[23] The temperature dependence of the peak energies and intensities of the NP lines are summarized in Fig. 1(b). The peak intensities increase with decreasing temperature. The peak energy location is almost constant above 50 K and decreases below 40 K. These peak shifts at low temperatures suggest that the excitons are localized in the shallow band-tail states,[17] which are caused by spatial fluctuations of the potential energy due to varying alloy compositions and interface roughness. The temperature dependence of the PL decay of the NP line is well correlated with its PL intensity dependence, as shown in Fig. 1(c): the PL decay rate increases as the PL intensity increases. The enhancement of the PL decay rate and intensity can be explained by enhancement of the radiative recombination process, not by thermal quenching of the PL intensity.

Figure 2(a) shows the time-integrated PL spectra obtained by varying the excitation intensity. The spectra are normalized according to the excitation intensities. The samples were kept at 10 K during the measurements. Broadening to the higher-energy side appears for all NP, TO, and TA lines. The excitation intensity dependence of the PL peak intensity and the peak energy of the NP line are shown in Fig. 2(b). Under low-density excitation (<0.1 J/cm^2), the PL intensity increases with excitation intensity (broken line). With increasing excitation density, however, the PL intensity begins to saturate while the PL peak energy is slightly blueshifted [Fig. 2(c)]. These phenomena are explained by the state filling of the localized exciton states, i.e., the saturation of localized exciton states and the redistribution of excitons to delocalized states.

Importantly, the observed PL intensity saturation under high excitation densities also marks the onset of the carrier-killing nonradiative recombination processes such as Auger recombination. In bulk Si and related materials, the Auger process is the dominant nonradiative recombination process
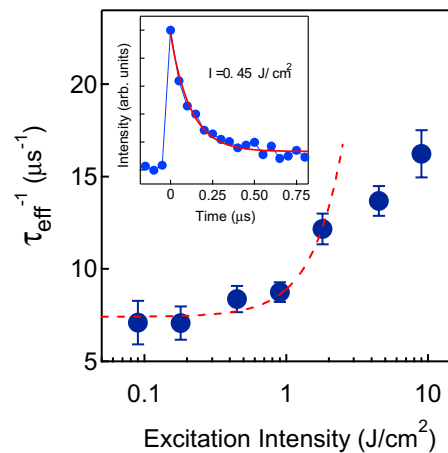

FIG. 3. (Color online) Dependence of the PL decay rate on excitation intensity in the Si$_{0.85}$Ge$_{0.15}$/Si superlattice. Inset: PL decay dynamics under 0.45 J/cm^2 excitation.

under high-density photoexcitation and/or in the presence of heavily doped electrically active impurities.[24] By taking into account the nonradiative Auger recombination, the PL intensity via radiative bimolecular recombination of carriers can be shown to depend on the excitation intensities: $I_{PL} \propto I_{exc}^{2/3}$ as shown by the solid line in Fig. 2(b). Moreover, an additional carrier reduction process, e.g., free-carrier absorption, will also lead to the further saturation of the PL intensity under the extreme high-density excitation.[9]

To clarify the dynamic aspects of the high-density excitation effects, the PL decay is measured as a function of the excitation intensity. The inset of Fig. 3 shows a typical result of NP line intensity decay dynamics measured at an excitation intensity of 0.45 J/cm^2. The decay rates are extracted by fitting the data with a single exponential function, as shown by the solid curve in the inset of Fig. 3. They are shown as a function of the excitation intensity. As can be seen, the PL decay rate increases with increasing excitation intensity. However, the PL decay rate decreases with temperature [Fig. 1(c)]. This indicates that lattice heating by intense excitation does not play a primary role in the PL decay dynamics. It is likely that the rapid decay is due to the nonradiative Auger decay processes that occur in high-density electron-hole systems.

In the nonradiative Auger recombination, the decay rate depends on the densities of electrons and holes. In the case of unbounded electrons and holes, the decay rate is proportional to the square of the electron-hole pair density, $\tau^{-1} \propto Cn^2$, where C is the Auger coefficient. From the observed increase in the decay rate in Fig. 3, the Auger coefficient can be estimated. We evaluate the number of photogenerated carriers in the SL structure immediately after femtosecond laser excitation using the number of incident photons and the volume of the confinement potential (or the total width of the quantum wells) in the SL. The excitation intensity of 1 J/cm^2 corresponds to a carrier density of $n=4 \times 10^{22}$ cm^{-3}. As shown by the broken line in Fig. 3, the Auger coefficient is extracted by fitting the power dependence of the decay rates below 2 J/cm^2, which corresponds to $C \sim 9 \times 10^{-40}$ cm^6 s^{-1}.
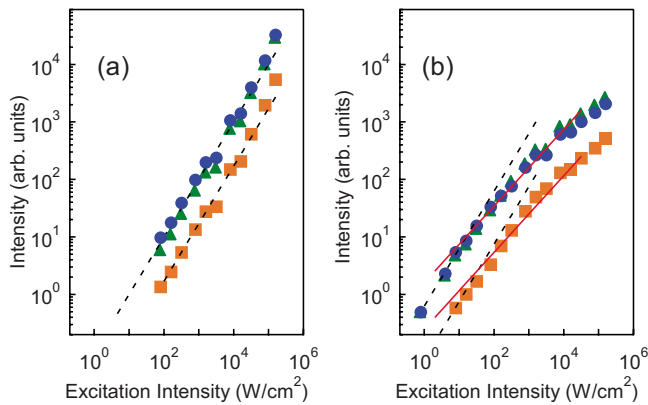
FIG. 4. (Color online) Dependence of the peak intensities of cw PL on excitation intensity for the NP (circle), TA (square), and TO (triangle) lines in (a) $Si_{0.85}Ge_{0.15}/Si$ superlattice and (b) $Si_{0.82}Ge_{0.18}/Si$ single-quantum well. The broken lines show the linear power dependence. The solid lines show the power dependence of the Auger-recombination-limited PL intensity ($I_{PL} \propto I_{exc}^{2/3}$).

Under high-density excitation, however, the initial carrier density is likely to be overestimated because the free-carrier absorption and nonlinear optical processes reduce the photogenerated carriers.[9] By taking account of the photocarrier reduction due to free-carrier absorption, we can roughly explain the departure of the experimental results from the fitting result at excitation intensities above 4 J/cm^2. As a matter of fact, such a reduction in carrier densities due to the free-carrier absorption is consistent with the strongly saturating behaviors of PL peak intensity ($I_{PL} \propto I_{exc}^m$, with $m < 2/3$), as visible in Fig. 2(b). The value of C estimated above can therefore be treated as a lower limit. It should be noted here that the magnitude of the Auger coefficient in the SL structure is much smaller than that in the bulk Si, which is approximately $C = 1 \times 10^{-31}$ cm^6 s^{-1}.[25] In contrast, the Auger coefficient in $Si_{1-x}Ge_x$ quantum wells is theoretically predicted to be much larger than that in Si crystals, reflecting the increase in transition probabilities in the former.[26] The reason for the small Auger coefficient in SL structures is discussed below.

To clarify the nature of the Auger recombination process in SL structures, we compare the dependence of the cw PL spectra on excitation intensity in SL and SQW structures. Under the same excitation and experimental conditions, the PL intensities of NP, TA, and TO lines were measured in both the SQW and SL. The samples were kept at 6 K during the measurements. When the excitation is weak, the PL lifetimes and peak intensities in both structures are similar. This indicates that in the SL, the magnitude of the oscillator strength is approximately equal to that in the SQW. As shown in Fig. 4(a), the PL intensity in the SL structure is approximately proportional to the excitation intensity up to 10^6 W/cm^2. In contrast, the PL intensities of the SQW saturate even at a weak photoexcitation of 10^2 W/cm^2 [Fig.

4(b)]. The excitation power dependence of the PL intensities follows the power law $I_{PL} \propto I_{exc}^{2/3}$, as shown by the solid lines. This nonlinear behavior indicates the presence of Auger recombination in the SQW structure, as discussed in Figs. 2 and 3, as opposed to the influence of amplified spontaneous emission (ASE) in the in-plane directions that further growth of the surface-emitting PL is hampered. ASE is insignificant under the experimental conditions studied in this particular set of indirect-gap samples. Based on the well periods of the quantum wells in the SL sample (99 pairs), the carrier sheet density (or carrier density in the well) is estimated to be 10^2-fold smaller than that in the SQW samples, where all wells in the SL sample are excited homogeneously. However, such a difference in the carrier density is not sufficient to explain the experimental results shown in Fig. 4. The difference between the two samples indicates that the Auger recombination in the SL structures is suppressed as opposed to the SQW structure.

The low Auger recombination rate in the SL structures is attributed to the delocalized states where the penetration of the carrier wave function into the Si barrier region becomes pronounced. The coupling between the carriers in the neighboring quantum wells results in delocalized states that have significant wave-function overlap into the silicon barrier layer.[22] The Auger rate in bulk Si is calculated to be smaller than that in the $Si_{1-x}Ge_x$ well layer.[26] Therefore, the delocalized carriers in the SL structure have a smaller Auger coefficient than the $Si_{1-x}Ge_x$ SQW. With an increase in the penetration of the carrier wave function into the Si barriers, the Auger in the $Si_{1-x}Ge_x$ SL rate is reduced and should become close to that in the bulk Si. The control of parameters in SLs, such as the coupling strength between single-quantum wells, allows us to control both the electronic structure and the dynamical many-body effects. Although strong Auger loss appears in nanostructures, such as the SQW, the Auger loss rate is suppressed and the PL efficiency is enhanced in the SL structure.

In conclusion, we studied photocarrier dynamics under high-density excitation in the $Si_{0.85}Ge_{0.15}/Si$ superlattice using time-resolved PL measurements. We observed the nonradiative Auger processes in the delocalized states. The Auger process in $Si_{1-x}Ge_x/Si$ SLs was more diminished than that in the $Si_{1-x}Ge_x/Si$ SQW even though the magnitude of the oscillator strength in the SLs is similar to that in the SQW. Given the different dependence of their PL intensity on excitation intensity, coupled nanostructures have a unique advantage for controlling carrier-carrier interactions, such as Auger recombination.

*Corresponding author; kanemitu@scl.kyoto-u.ac.jp

[1] L. T. Canham, Appl. Phys. Lett. **57**, 1046 (1990).

[2] *Towards the First Silicon Laser*, edited by L. Pavesi, S. Gaponenko, and L. D. Negro (Kluwer Academic, Dordrecht, 2003).

[3] Y. Kanemitsu, Phys. Rep. **263**, 1 (1995).

[4] Y. Kanemitsu, J. Lumin. **100**, 209 (2002).

[5] L. Pavesi, L. D. Negro, C. Mazzoleni, G. Franzò, and F. Priolo, Nature (London) **408**, 440 (2000).

[6] W. L. Ng, M. A. Lourenço, R. M. Gwilliam, S. Ledain, G. Shao, and K. P. Homewood, Nature (London) **410**, 192 (2001).

[7] S. G. Cloutier, P. A. Kossyrev, and J. Xu, Nature Mater. **4**, 887 (2005).

[8] J. S. Biteen, D. Pacifici, N. S. Lewis, and H. A. Atwater, Nano Lett. **5**, 1768 (2005).

[9] H. Rong, A. Liu, R. Jones, O. Cohen, D. Hak, R. Nicolaescu, A. Fang, and M. Paniccia, Nature (London) **433**, 292 (2005).

[10] K. Dohnalová, I. Pelant, P. Gilliot, O. Crégut, and B. Hönerlage, Appl. Phys. Lett. **88**, 251105 (2006).

[11] M. Tajima and S. Ibuka, J. Appl. Phys. **84**, 2224 (1998).

[12] N. Pauc, V. Calvo, J. Eymery, F. Fournel, and N. Magnea, Phys. Rev. Lett. **92**, 236802 (2004).

[13] S. Nihonyanagi and Y. Kanemitsu, Appl. Phys. Lett. **85**, 5721 (2004).

[14] H. Htoon, J. A. Hollingsworth, R. Dickerson, and V. I. Klimov, Phys. Rev. Lett. **91**, 227401 (2003).

[15] V. I. Klimov, S. A. Ivanov, J. Nanda, M. Achermann, I. Bezel, J. A. McGuire, and A. Piryatinski, Nature (London) **447**, 441 (2007).

[16] L. Huang and T. D. Krauss, Phys. Rev. Lett. **96**, 057407 (2006).

[17] J. C. Sturm, H. Manoharan, L. C. Lenchyshyn, M. L. W. Thewalt, N. L. Rowell, J.-P. Noël, and D. C. Houghton, Phys. Rev. Lett. **66**, 1362 (1991).

[18] A. Zrenner, B. Fröhlich, J. Brunner, and G. Abstreiter, Phys. Rev. B **52**, 16608 (1995).

[19] L. C. Lenchyshyn, M. L. W. Thewalt, D. C. Houghton, J.-P. Noël, N. L. Rowell, J. C. Sturm, and X. Xiao, Phys. Rev. B **47**, 16655 (1993).

[20] S. Fukatsu, H. Yoshida, N. Usami, A. Fujiwara, Y. Takahashi, Y. Shiraki, and R. Ito, Jpn. J. Appl. Phys., Part 2 **31**, L1319 (1992).

[21] X. Xiao, C. W. Liu, J. C. Sturm, L. C. Lenchyshyn, and M. L. W. Thewalt, Appl. Phys. Lett. **60**, 1720 (1992).

[22] S. Fukatsu and Y. Shiraki, Appl. Phys. Lett. **63**, 2378 (1993).

[23] D. J. Robbins, L. T. Canham, S. J. Barnett, A. D. Pitt, and P. Calcott, J. Appl. Phys. **71**, 1407 (1992).

[24] P. T. Landsberg, *Recombination in Semiconductors* (Cambridge University Press, Cambridge, 1991).

[25] J. Dziewior and W. Schmid, Appl. Phys. Lett. **31**, 346 (1977).

[26] E. Corbin, C. J. Williams, K. B. Wong, R. J. Turton, and M. Jaros, Superlattices Microstruct. **19**, 25 (1996).